Single-photon Imaging Inspired by Human Vision

Hooman Mohseni
Bio-inspired Sensors and Optoelectronics Laboratory (BISOL)
Department of Electrical Engineering and Computer Sciences
Northwestern University, Evanston, IL 60208
Email: hmohseni@eecs.northwestern.edu
URL: www.bisol.northwestern.edu

ABSTRACT

Single photon detectors are regarded as a key enabling technology in a wide range of medical, industrial, and military applications. However, the existing single photon detectors that can operate at or near room temperature have poor efficiency and high noise. Interestingly, the counterparts of these devices in nature, namely the rod cells, have amazingly high efficiency and low noise. In particular, the noise performance of the rod cells is five to six orders of magnitude better than the semiconductor based single photon detectors at room temperature. At Bio-inspired Sensors and Optoelectronics Laboratory, we explored the origin of such a high noise performance, and designed and implemented a novel semiconductor device based on the underlying detection mechanism in the rod cells. Our device shows very promising properties including orders of magnitude higher gain and lower noise compared with the existing devices. More interestingly, the low operating voltage of the device combined with high gain uniformity should allow, for the first time, realization of large imaging arrays with a high internal gain. Such imagers would open new opportunities for novel applications such as quantum ghost imaging.

Keyword: Single Photon Detectors, Infrared Detector, Nano-processing, Single Electron Transistor, Bio-inspired

BACKGROUND

Compact solid-state single photon detectors are regarded as enabling components in a wide range of applications such as biophotonics, tomography, homeland security, non-destructive material inspection, astronomy, quantum key distribution, and quantum imaging. However, these devices are quickly becoming the bottleneck in many applications due to their limited stable gain of less than a few hundreds[1], low quantum efficiency[Error! Bookmark not defined.,2], high excess noise[3,4], and long deadtime[5,6]. These problems have encouraged research on alternative detection methods based on superconductors[7,8], and quantum dots[9,10]. Although these methods can potentially alleviate a large number of problems associated with avalanche-based SPDs, they require extremely low operating temperatures, usually below 4°K, which prevent their practical utilization in many applications.

Inspired by the amazing sensitivity of the rod cells, we designed and implemented a novel semiconductor base detector detailed in this paper. Rod cell is an extremely sensitive light sensor, and is capable of detecting a few photons[11]. Rod cells are made of inner and outer segments, among which a steady current flow due to Na^+ and K^+ transport in dark. 0-a shows the overall detection mechanism in the rod cells schematically. Outer segment is very rich in photosensitive rhodopsin molecule, which is a strong absorber of photons with peak sensitivity in blue-green spectrum. Upon light reception rhodopsin is triggered with structural changes and acts as a catalyst. Activated rhodopsin triggers a chain of reactions that lead to the destruction of chemical messenger cyclic guanosine monophosphate (cGMP). Finally, the transport channels for Na^+ and K^+ respond quickly to any change in cGMP concentration by closing the ion channels, and significantly changing the current passing through the rod cell. The significance of this detection mechanism is that it can provide both high efficiency and high sensitivity at room temperature; a condition that is very difficult to achieve in conventional single photon detectors. Simply put, the energy of a single photon in the visible or short infrared is extremely small, less than one atto Joule, and the only reliable way to sense this small energy is to use a very small volume, for example a quantum dot[10]. However, the wavelength of light is significantly larger than such a sensor, and hence the interaction between the photon and the sensor, or quantum efficiency, is extremely small. Any attempt to enhance the efficiency by increasing the volume would simply reduce the sensitivity. Rod cell's detection mechanism

Human Vision and Electronic Imaging XIII, edited by Bernice E. Rogowitz, Thrasyvoulos N. Pappas,
Proc. of SPIE-IS&T Electronic Imaging, SPIE Vol. 6806, 680604, © 2008 SPIE-IS&T · 0277-786X/08/$18

resolves this conflict by using a micron-scale absorbing volume, the outer cell, and nano-scale sensing elements, or the ion channels.

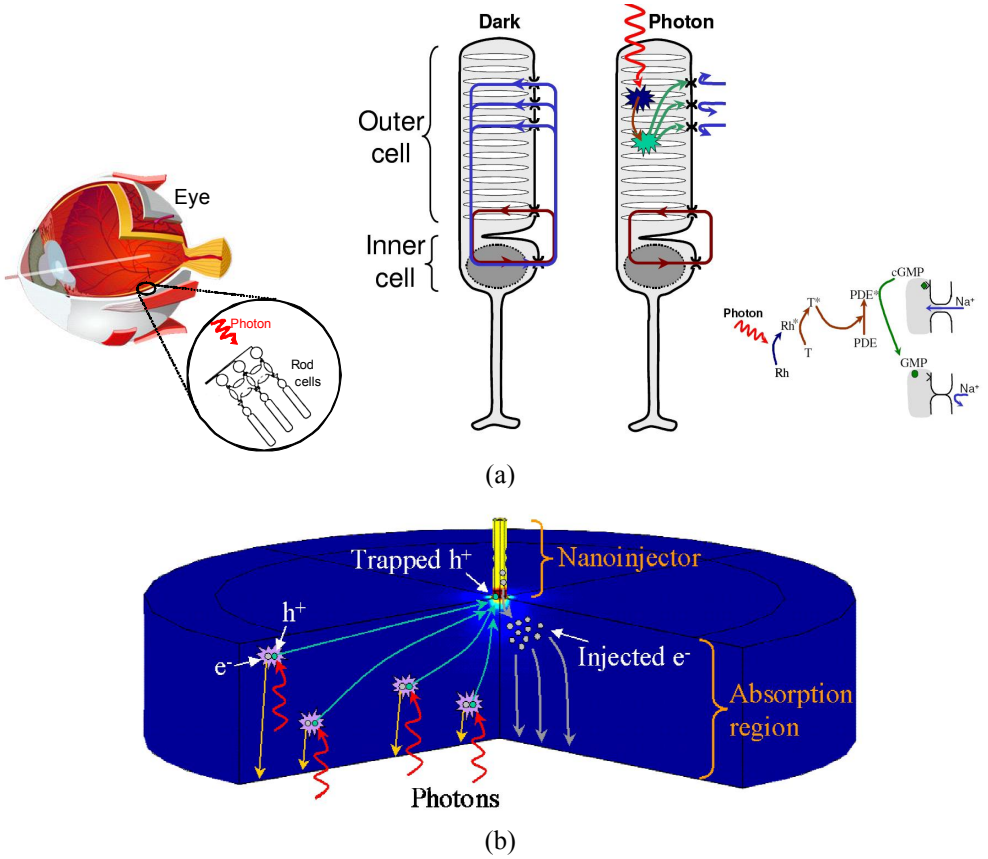

Figure 1. The detector concept inspired by the detection mechanism in rod cells. (a) Photon detection process in the rod cells involves light absorption in a micron-scale absorbing volume, the outer cell, and nano-scale sensing elements, or the ion channels (b) Schematic of our semiconductor base single photon detector showing the large absorption region, and the nanoinjector. The ultra small volume of the hole trap makes the device sensitive to a single charge.

DEVICE CONCEPT:

We incorporated these principles in our novel semiconductor platform. 0-b shows the principle of photon detection process in our device. Upon absorption, photons generate an electron-hole pair in the large absorption region. The electron and hole are immediately separated because of the internal electric field. Holes are attracted to the nano-injector that has a type-II band alignment and presents a trap for holes. A single photo-generated hole in the absorption region is equivalent to a charge density of 1.4×10^{-3} C/m^3. However, when trapped inside the 50 nm thick by 100 nm wide nano-injector, the same hole creates a charge density of more than 400 C/m^3. Therefore, the impact of the hole increases by more than 5 orders of magnitude. Equivalently, the small volume of the trap represents an ultra-low capacitance, and hence the entrapment of a single hole leads to a large change of potential and produces an amplified electron injection similar to the process in single electron transistors (SET)[12]. Detailed simulations and potential calculations show that a single hole can alter the potential by more than 52 mV. This value is significantly higher than the thermal fluctuation energy of carriers at 300ºK, and hence a high signal to noise ratio is possible even at room temperature.

DEVICE DESIGN AND PROCESSING:

We used a three-dimensional simulation model to design the epitaxial layer thickness, doping level, and composition. The layers are grown using conventional epitaxial growth on InP substrates, and the devices are processed as detailed in the following. The detector has three main layers: InP injection reservoir, GaAsSb entrapment/barrier layer and InGaAs absorption volume. It relies on focalization and nanoinjection of carriers: When photons reach the large absorbing medium, electron-hole pairs are generated by optical excitation. The geometry of the device is designed such that the holes from the whole absorption volume are focused into the smaller nanoinjector, resulting in the focalization process. The of the nanoinjector tip is made of GaAsSb with type-II band alignments to both other layers, and presents a trap for incoming holes and a barrier for electrons. Furthermore, the extremely small volume of GaAsSb ensures an ultra-low capacitance. Focalized carriers alter the potential of the nano-injector tip significantly due to the ultra-low capacitance. Any increase in the nano-injector potential leads to an exponential increase in electron injection towards the InP substrate and the back contact.

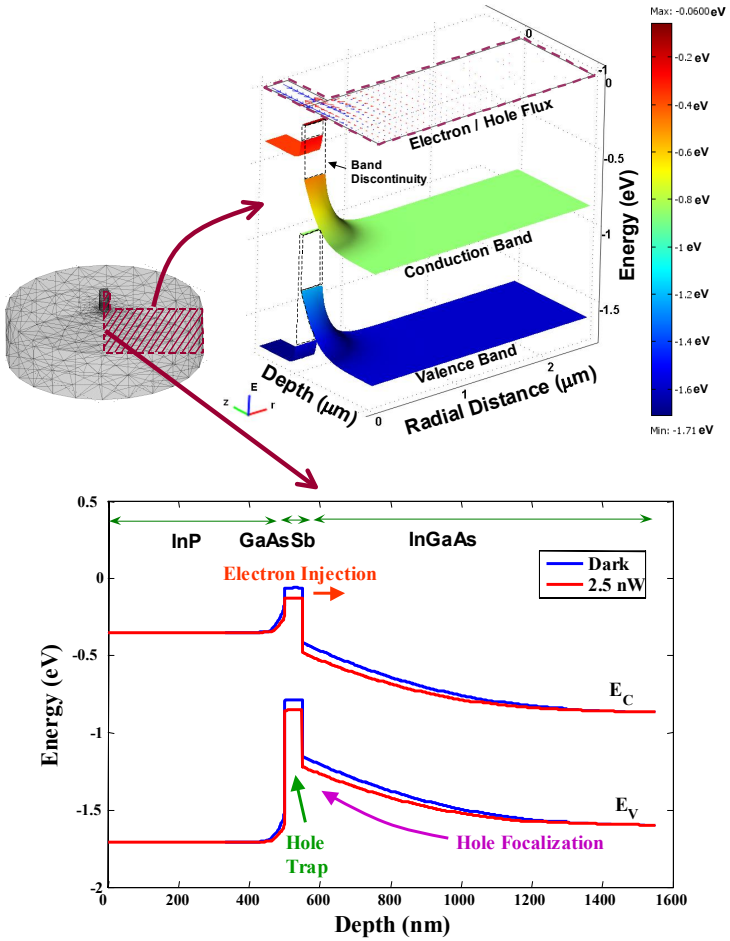

Figure 2. Upper image shows the valence and conduction band energies as a function of radial distance and depth for a device biased at 0.6 volt. The electron (blue arrows) and hole (red arrows) flow rate densities are also projected on the cross-section plane. Lower image shows the band structure along the radial axis of the device biased at 0.6 volts with (red lines) and without (blue lines) optical illumination. Note that upon illumination, holes are attracted to the nanoinjector and the potential of GaAsSb volume at the tip of nanoinjector increases due to the trapped holes. This increased potential lowers the conduction band barrier and increases electron injection.

The samples were grown on n-doped InP substrates with n~$3x10^{18}$ cm^{-3}. Wafers were patterned with e-beam lithography (EBL) to form nanometer size pillars. Conventional metallization with e-beam evaporation was used to form multi-layer metal contacts. Etching process consisted of dry etching with methane and hydrogen in a reactive ion etcher (RIE), followed by a mild wet etching with sulfuric acid and hydrogen peroxide. Samples were passivated and planarized with polyimide to provide planar surfaces for metal contact pads. Photolithography was used to produce liftoff patterns.

Final metallization was used to form reliable top contacts to the submicron features. The processing yielded more than 25 units (dies) on a quarter 2" wafer. Each die consists of arrays of devices with metal contact pads, in addition to hundreds of individual devices.

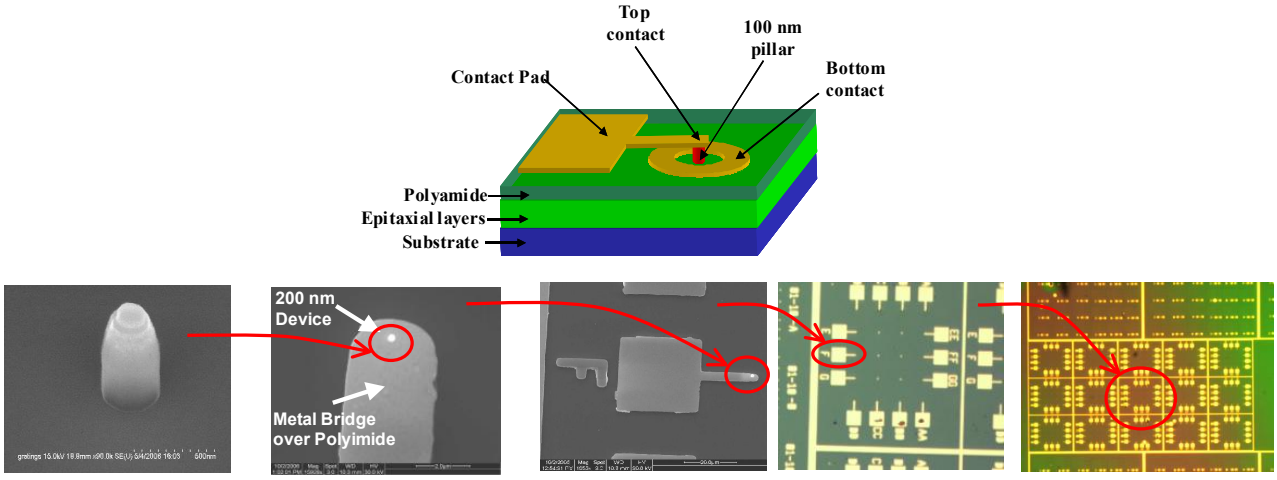

Figure 3. The top figure shows the schematic structure of a planarized 100nm detector with metal contact pad. The bottom series show images from a single nanopillar to arrays of fully processed devices. From left to right: 200 nm nanopillar; planarized 200 nm pillar covered with metal bridge; metal contact pad and the bridge connecting the pillar; a cell containing 14 devices with metal pads; an array of 15 cells on a single die.

MEASUREMENT RESULTS:

Fabricated devices are tested using computerized setups. The measured dark current shows a fairly good agreement with the modeling results, considering that we did not fit any parameter (Figure 4-a). The gain of the device increases with the device bias, and beyond ~1 volt the device shows a stable gain of more than several thousand (Figure 4-b). Compared to existing avalanche-based detectors, our devices show more than an order of magnitude higher stable gain, and much better dark current values. Also, despite such a high gain our device shows a very uniform spatial response (see Figure 4-c). We believe that the low internal electric field in our devices is the main reason for the observed uniformity. The measured response decreases rapidly beyond a radius of about 8 μm by orders of magnitude, in complete agreement with our model. This property suggests that two-dimensional arrays of such detectors might not need pixel isolation methods such as ion implantation or mesa etching.

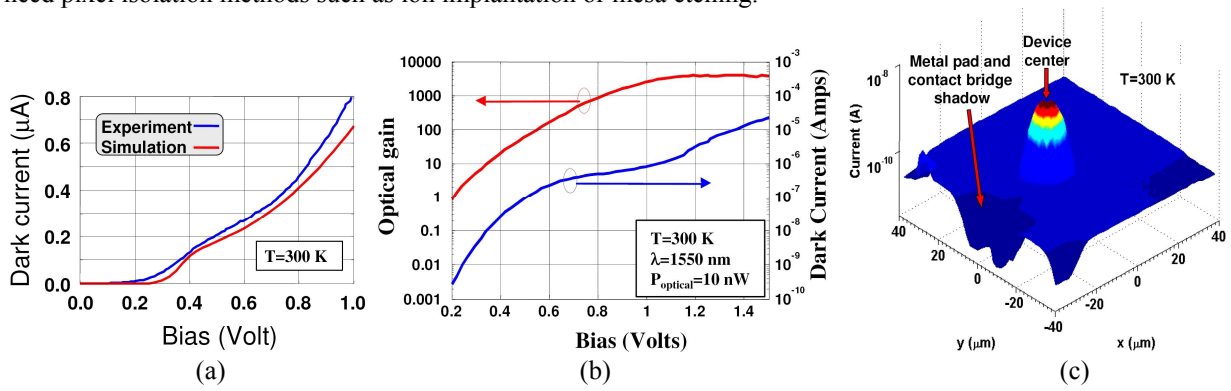

Figure 4. Measured dark current, gain, and spatial response. a) Measured and modeled dark current of a device at room temperature show relatively good agreement. All model parameters were obtained from published literature. b) Measured dark current and gain of a device at room tempertaure and for an illumination power of 10 nW at λ=1550 nm. The gain is almost independent of the optical power below 10 nW. c) Spatial photoresponse of the device is uniform up to nearly 8 μm, beyond which the response decreases rapidly.

Transient response of the detector was tested with a pulsed laser with a pulse width of 300 fs. Calibrated attenuators were used to reduce the light intensity. Figure 5-a shows the averaged time response of the device to a low photon rate pulse train. The measurement shows high sensitivity and speed, as well as a negligible deadtime, as predicted by our simulation. Figure 5-b shows the measured noise performance of the device at room temperature. The device shows an excess noise factor that is less than unity up to a gain of 4000. This performance is in stark contrast with conventional APD, where excess noise factor grows rapidly with gain, and noise is tens of times higher than the shot noise limit at gain values below 100. More importantly, we have measured excess noise factors that are consistently below unity, indicating shot noise suppression in our devices. Such behavior might be resulted from the nano-injector, since shot noise suppression has been predicted theoretically[13] and measured experimentally[14,15] in similar structures.

Noise equivalent power (NEP) of our detector is calculated from measured dark and photocurrent to be about $2x10^{-16}$ W/Hz^{½}. The responsivity is more than 4000 A/W at 1550 nm at 300ºK. As a comparison, the best avalanche photodetectors have NEP values larger than $2x10^{-15}$ watt/Hz^{½} and stable responsivity of about 30 A/W at room temperature[16,17].

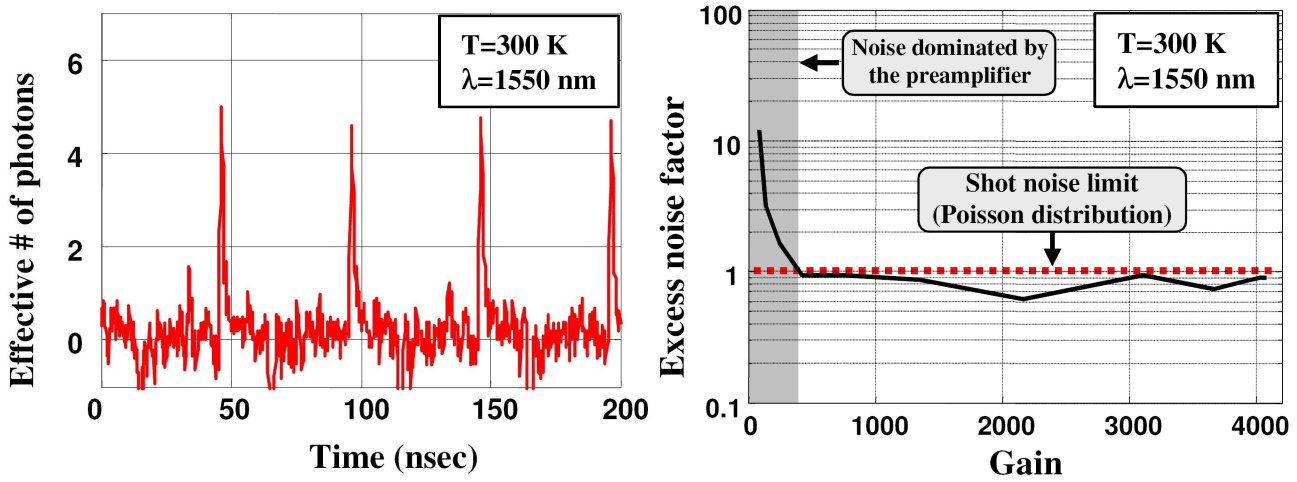

(a) (b)

Figure 5. Measured time response and noise performance. a) Time response of the device at λ=1550 nm at room temperature shows a fast rise time of about 1 nsec. The deadtime is very short, and the device is ready for new detection only a few nanoseconds after each detection events. b) Measured excess noise factor of a device as a function of internal gain shows below shot-noise limit performance up to very high gain values.

CONCLUSION:

These results show orders of magnitude improvement in sensitivity, gain, and deadtime compared with the existing APD at similar wavelength and temperature. Although our devices have a cutoff wavelength of 1.7 μm, the underlying concept can be used to improve photon detectors with cutoff wavelengths from UV to far infrared.

ACKNOWLEDGEMENT:

The majority of the nano-processing part of this work was performed at the University of Illinois at Urbana-Champaign, and under supervision of professor Ilesanmi Adesida. This work is partially funded through NSF CAREER Award, and Photon Counting Array program at DARPA-MTO.

REFERENCES:

[1] Duan, N. et al. Detrimental effect of impact ionization in the absorption region on the frequency response and excess noise performance of InGaAs-InAlAs SACM avalanche photodiodes. *IEEE Journal of Quantum Electronics* **41**, 568-572 (2005).

[2] Bourennane, M., Karlsson, A., Ciscar, J. P. & Mathes, M. Single-photon counters in the telecom wavelength region of 1550 nm for quantum information processing. *Journal of Modern Optics* **48**, 1983-1995 (2001).
[3] Mcintyre, R. J. Multiplication Noise in Uniform Avalanche Diodes. *IEEE Transactions on Electron Devices* **13**, 164-168 (1966).
[4] Duan, N. et al. High-speed and low-noise SACM avalanche photodiodes with an impact-ionization-engineered multiplication region. *IEEE Photonics Technology Letters* **17**, 1719-1721 (2005).
[5] Ribordy, G. g. et al. Photon counting at telecom wavelengths with commercial InGaAs/InP avalanche photodiodes: current performance. *Journal of Modern Optics* **51**, 1381-1398 (2004).
[6] Cova, S., Ghioni, M., Lotito, A., Rech, I. & Zappa, F. Evolution and prospects for single-photon avalanche diodes and quenching circuits. *Journal of Modern Optics* **51**, 1267-1288 (2004).
[7] Mather, J. C., Astronomy - Super photon counters. *Nature* **401**, 654-655 (1999).
[8] Rosenberg, D., Lita, A. E., Miller, A. J., Nam, S. & Schwall, R. E. Performance of photon-number resolving transition-edge sensors with integrated 1550 nm resonant cavities. *Applied Superconductivity, IEEE Transactions on* **15**, 575-578 (2005).
[9] Hashiba, H., Antonov, V., Kulik, L., Komiyama, S. & Stanley, C. Highly sensitive detector for submillimeter wavelength range. *Applied Physics Letters* **85**, 6036-6038 (2004).
[10] Komiyama, S., Astafiev, O., Antonov, V., Kutsuwa, T. & Hirai, H. A single-photon detector in the far-infrared range. *Nature* **403**, 405-407 (2000).
[11] Hecht, S., Shlaer, S. & Pirenne, M. H. Energy, quanta, and vision. *Journal of. Gen. Physioogy* **25**, 819-840 (1942).
[12] Devoret, M. H. & Schoelkopf, R. J., Amplifying quantum signals with the single-electron transistor. *Nature* **406**, 1039-1046 (2000).
[13] Reklaitis, A., & Reggiani, L. Shot noise suppression from independently tunnelled electrons in heterostructures. *Semiconductor Science and Technology* **14**, L5-L10 (1999).
[14] Aleshkin, V.Y. et al, Giant suppression of shot noise in double barrier resonant diode: a signature of coherent transport. *Semiconductor Science and Technology* **18**, L1-L4, (2003).
[15] Iannaccone, G., Lombardi, G. , Macucci, M., & Pellegrini, B. Enhanced shot noise in resonant tunneling: theory and experiment. *Physical Review Letters* **80**, 1054-1057, (1998).
[16] Voss, P. L., Koprulu, K. G., Choi, S. K., Dugan, S. & Kumar, P. 14MHz rate photon counting with room temperature InGaAs/InP avalanche photodiodes. *Journal of Modern Optics* **51**, 1369-1379 (2004).
[17] Pellegrini, S. et al. Design and performance of an InGaAs-InP single-photon avalanche diode detector. *Quantum Electronics, IEEE Journal of* **42**, 397-403 (2006).